Materials Today Communications 52 (2026) 114947

Contents lists available at ScienceDirect

Materials Today Communications

journal homepage: www.elsevier.com/locate/mtcomm

Investigating thermal insulation in bio-derived cellulose fiber reinforced aerogels: Microscale modeling and RSM optimization approach

Wiem Nasri [a], Sondes Ifa [a], Marwa Hannachi [a], Mabrouk Mosbahi [a,b,c,*], Ridha Djebali [d], Khaled Gammoudi [a,c], Tullio Tucciarelli [b], Abderazak Bezazi [e], Paulo N.B. Reis [f], Zied Driss [a,g]

[a] *Laboratory of Electro-Mechanic Systems (LASEM), National School of Engineers of Sfax (ENIS), University of Sfax (US), B.P. 1173, Road Soukra km 3.5, Sfax 3038, Tunisia*
[b] *University of Palermo, Department of Engineering, 90128, Italy*
[c] *Department of Mechanical Engineering, Higher Institute of Applied Sciences and Technology of Gafsa, University of Gafsa, Gafsa 2112, Tunisia*
[d] *UR: Modeling, Optimization and Augmented Engineering, ISLAI Béja, University of Jendouba, Béja 9000, Tunisia*
[e] *Laboratory of Applied Mechanics of New Materials (LMANM), University May 08, 1945, B.P. 401, Guelma 24000, Algeria*
[f] *University of Coimbra, CEMMPRE, ARISE, Department of Mechanical Engineering, Coimbra 3030-780, Portugal*
[g] *Department of Mechanical Engineering, Faculty of Engineering, University of Tabuk, Tabuk, Saudi Arabia*

A R T I C L E I N F O

Keywords:
Cellulose fiber reinforced aerogel (CFRA)
Micromechanical modeling
FEM
Response surface methodology (RSM)
Box–Behnken design (BBD) and Thermal insulation composites

A B S T R A C T

Cellulose fiber reinforced aerogel (CFRA) composites are emerging as sustainable super-insulating materials by integrating bio-based cellulose fibers within a silica aerogel matrix, which enhances structural stability while maintaining low thermal conductivity (TC). This study presents a computational framework that predicts and optimizes the effective thermal conductivity (ETC) of CFRA composites using a combination of micromechanical modeling and statistical analysis. A three-dimensional periodic representative volume element (RVE) was developed to simulate steady-state heat conduction, and a Box–Behnken design (BBD) with Response Surface Methodology (RSM) was implemented to model the impact of microstructural parameters. The predictive model, validated against analytical and experimental data, demonstrated excellent accuracy, with a coefficient of determination $R^2 = 0.9976$, adjusted $R^2 = 0.9948$). Sensitivity analysis revealed that temperature and aerogel TC are the predominant factors influencing ETC, while fiber radius has minimal effect within the studied range (< 0.1% variation). An optimal configuration with a fiber radius of 7 µm, fiber volume fraction of 1.3%, and aerogel conductivity of 0.016 $W \cdot m^{-1} \cdot K^{-1}$, yielding an ETC of 0.0163 $W \cdot m^{-1} \cdot K^{-1}$ at room temperature, which is 37% lower than the TC of air (0.026 $W \cdot m^{-1} \cdot K^{-1}$). This integrated modeling-optimization framework offers an effective tool for designing and optimizing sustainable CFRA insulation materials.

1. Introduction

Thermal insulation materials play a critical role across multiple industrial sectors, including building construction, refrigeration, aerospace, and cryogenic systems [1–4]. Their primary function is to limit heat transfer and preserve temperature gradients between different regions, thereby improving energy efficiency, reducing operational costs, and enhancing occupant comfort. As global concerns regarding energy consumption and environmental sustainability intensify, the demand for advanced, lightweight, and high-performance insulating materials has grown substantially. In this context, nanostructured materials, particularly aerogels and bio-based composites, have emerged as highly promising candidates for next-generation insulation systems. Recent studies have emphasized the integration of statistical optimization [5–7] and sustainable processing routes to enhance the multifunctional performance of fiber-reinforced composites, reflecting the broader trend toward eco-efficient composite development [8,9].

Among these materials, cellulose fiber reinforced aerogel (CFRA) composites represent a particularly attractive class due to their combination of biodegradability, mechanical flexibility, and low TC. CFs,

* Corresponding author at: Laboratory of Electro-Mechanic Systems (LASEM), National School of Engineers of Sfax (ENIS), University of Sfax (US), B.P. 1173, Road Soukra km 3.5, Sfax 3038, Tunisia.

E-mail addresses: wiem.nasri@enis.tn (W. Nasri), sondes.ifa@enis.tn (S. Ifa), marwa.hannachi@enis.tn (M. Hannachi), mabrouk.mosbahi@unipa.it (M. Mosbahi), ridha.djebali@islaib.u-jendouba.tn (R. Djebali), gammoudy@gmail.com (K. Gammoudi), tullio.tucciarelli@unipa.it (T. Tucciarelli), bezazi.abderrezak@gmail.com (A. Bezazi), paulo.reis@dem.uc.pt (P.N.B. Reis), zied.driss@enis.tn (Z. Driss).

https://doi.org/10.1016/j.mtcomm.2026.114947
Received 11 December 2025; Received in revised form 24 February 2026; Accepted 2 March 2026
Available online 4 March 2026

sourced from wood pulp, cotton, hemp, and other plant-based materials, are increasingly utilized in bio-composites thanks to their renewable nature, excellent mechanical properties, and environmental compatibility [10]. Cellulose-based composites have already demonstrated their versatility across fields such as water purification, sustainable construction, agricultural technologies, and packaging applications [11–14].

Aerogels themselves are exceptional mesoporous materials characterized by ultra-low density, high porosity (often exceeding 90–99%), and TC values ranging from 0.012 to 0.03 $W \cdot m^{-1} \cdot K^{-1}$ [15,16]. These properties make them ideal for cutting-edge applications such as gas storage, energy storage devices, drug delivery, catalysis, aerospace structures, and thermal insulation systems [17–22]. However, the intrinsic brittleness associated with their highly porous framework severely restricts their mechanical reliability during handling or under load. Consequently, improving the mechanical performance of aerogels without sacrificing their thermal insulation capability remains a key challenge. To address this limitation, researchers have highlighted both the potential of hybrid reinforcement strategies combining cellulose nanofibers, bio-derived binders, and hierarchical pore tailoring to improve strength and thermal stability while maintaining ultra-low conductivity [23–26], as well as the critical importance of fiber-matrix interactions in determining overall composite performance [27].

Building on these concepts, researchers have explored reinforcing aerogels with nanofibrillated cellulose (NFC) or coagulated cellulose networks. Two main fabrication strategies exist: (i) dispersing NFC directly into a silica sol, and (ii) impregnating silica sols into pre-coagulated cellulose matrices. When NFC is dispersed in silica sol, the resulting composites exhibit thermal conductivities between 0.014 and 0.015 $W \cdot m^{-1} \cdot K^{-1}$, comparable to traditional silica aerogels. In contrast, hydrophobized coagulated cellulose–silica aerogels can achieve thermal conductivities slightly lower than air (≈0.021–0.022 $W \cdot m^{-1} \cdot K^{-1}$) [28]. Despite these variations, the silica phase remains the dominant contributor to super-insulating behavior, while cellulose primarily enhances structural resilience.

Most cellulose-based aerogels reported in the literature are derived from cellulose I or cellulose II microstructures. While NFC aerogels can achieve exceptional thermal conductivities around 0.018 $W.m^{-1}.K^{-1}$, cellulose II-based aerogels generally show inferior insulation performance, with higher conductivity values and less favorable pore structures [29,30]. Jaxel et al. [31] compared two classes of cellulose silica aerogels synthesized through different ambient pressure drying (APD) techniques. Freeze-dried TEOS-cellulose nanofibril composites exhibited a high compressive modulus of 5.4 MPa and thermal conductivities between 0.016 and 0.018 $W \cdot m^{-1} \cdot K^{-1}$, significantly lower than previously reported values (≈0.023 $W \cdot m^{-1} \cdot K^{-1}$) [32]. Conversely, APD sodium-silicate aerogels reinforced with nonwoven silica fibers showed weaker mechanical performance (0.3–0.5 MPa) and displayed increasing TC with increasing fiber content (0.02–0.03 $W \cdot m^{-1} \cdot K^{-1}$), highlighting the sensitivity of aerogel performance to microstructural design.

Although substantial progress has been achieved in the development of cellulose-reinforced aerogels, most reported studies remain primarily experimental, concentrating on fabrication methods, structural characterization, and measured thermal conductivity values. While these works have significantly advanced the understanding of structure property relationships, they generally do not provide predictive frameworks capable of systematically assessing the influence of microstructural parameters on ETC. As a result, the ability to quantitatively evaluate and optimize design variables remains limited.

The present study aims to fill this gap by combining experimental insights from the literature with advanced computational modeling. FEA offers the ability to evaluate the thermal response of unidirectional (UD) CFRA laminae under controlled conditions and to explicitly analyze the influence of parameters such as fiber diameter, volume fraction and aerogel conductivity.

Furthermore, optimization studies specifically targeting the thermo-mechanical performance of CFRA composites are notably scarce. Although statistical design and response surface methodologies have been widely applied in other classes of fiber-reinforced composites, their integration with micromechanical thermal modeling for cellulose aerogel systems has not been extensively explored. A combined computational statistical approach could therefore provide a systematic means of quantifying parameter interactions and identifying optimal microstructural configurations.

To address this need, a predictive regression model using RSM based on a BBD is developed. The developed regression model quantifies the interaction effects between key microstructural variables and enables reliable prediction of ETC across various CFRA configurations. By coupling micromechanical simulation with statistical optimization, the proposed approach provides a systematic basis for evaluating thermal transport and identifying parameter combinations that enhance insulation performance.

In summary, this study aims to investigate the thermal behavior of unidirectional CFRA composites through a microscale computational framework integrated with RSM-based optimization. This integrated framework not only enables systematic parameter exploration within conduction-dominated regimes but also provides predictive insights and actionable design guidelines for enhancing the thermal efficiency of CFRA materials.

2. Methodology

To ensure the reliability and accuracy of the micromechanical predictions, a detailed three-dimensional RVE was developed using COMSOL Multiphysics (Version 5.2a). The software was selected due to its robustness in solving heat conduction problems with periodic boundary conditions and its suitability for three-dimensional RVE-based homogenization analysis. The RVE consists of a tetragonal unit cell of dimensions $0.1088 \times 0.1088 \times 2\ mm^3$, containing a single CF embedded within a silica aerogel matrix, as illustrated in Fig. 1.

The selection of cellulose fibers as reinforcement was motivated by three key factors: (1) their renewable and biodegradable nature, aligning with sustainability objectives; (2) their low intrinsic thermal conductivity, which minimizes thermal penalty compared to synthetic fibers; and (3) their mechanical flexibility, which can enhance composite toughness without introducing brittleness. The silica aerogel matrix was chosen for its ultra-low thermal conductivity and high porosity, which are essential for achieving super-insulating performance. The fiber diameter of 14 μm was selected based on the morphological characterization reported by Jaxel et al. [31], who measured the actual dimensions of cellulose fibers used in experimentally fabricated composites, ensuring that our model dimensions correspond to physically realizable materials. This value corresponds to a fiber volume fraction Vfy of 1.3% within the modeled unit cell.

A square array configuration was adopted for the fiber arrangement, providing a periodic and geometrically consistent representation of UD fiber-reinforced composites while allowing flexible variation of geometric parameters. Thermal properties of both constituents are reported in Table 1. Although the intrinsic thermal conductivity of cellulose and silica aerogels is known to vary with temperature, the present analysis assumes constant material properties within the investigated range (ambient to 200 °C). In this temperature interval, conductivity variations are generally gradual prior to degradation. Given the comparative and parametric nature of the study, this assumption enables isolation of microstructural effects on effective thermal conductivity (ETC). The potential influence of temperature-dependent properties may be addressed in future extensions of the model.

Due to the strong contrast between the thermal conductivities of cellulose fibers and silica aerogel, and the unidirectional alignment of the reinforcement, the resulting composite exhibits anisotropic thermal behavior. This anisotropy naturally arises from the heterogeneous

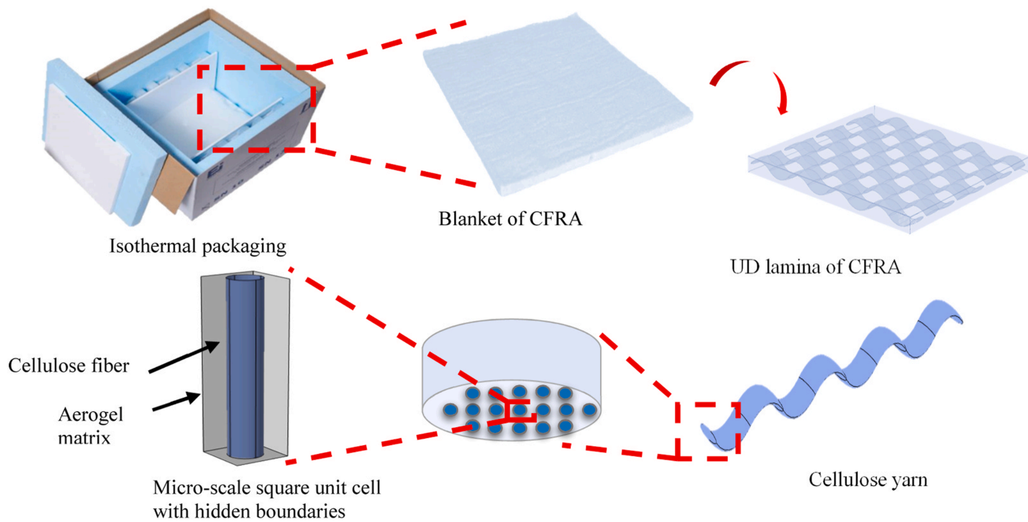

Fig. 1. Schematic configuration.

Table 1
Physical properties at room temperature (T = 25 °C).

Property	Cellulose fiber	Aerogel	Unit
Thermal conductivity	0.04 [40]	[0.014–0.023]	$W.m^{-1}.K^{-1}$
Density	1500 [40]	100	$Kg.m^{-3}$
Heat capacity at constant pressure	1600 [41]	1000	$J.kg^{-1}.K^{-1}$

microscale architecture and is reflected in the distinct ETC components obtained along the three local coordinate directions of the RVE. The RVE was periodically translated to represent the full UD lamina, enabling the computation of homogenized composite properties. This approach ensures that the predicted macroscopic behavior accurately captures the influence of fiber geometry, volume fraction and directional heat transfer mechanisms present at the microscale.

The present microscale model considers steady-state conductive heat transfer within the composite RVE. All simulations were conducted under steady-state conditions with the following ambient parameters: relative humidity was assumed to be 0% (dry conditions) as moisture effects were not considered in this study; ambient pressure was 1 atm; and initial temperature was set to 293.15 K, which served as the reference baseline for the parametric studies. The convergence criterion for the iterative solver was set to 10^{-6} for the temperature field.

Radiative heat transfer and gas-phase Knudsen effects inside aerogel nanopores are not explicitly modeled because within the investigated temperature range (30–200 °C), conduction remains the dominant transport mechanism in silica aerogels as reported in previous studies [33]. Radiative effects become increasingly relevant at substantially higher temperatures. This assumption is consistent with conduction-dominated homogenization approaches commonly adopted in finite-element modeling of composite insulation materials.

Additionally, perfect thermal contact between fiber and aerogel matrix is assumed, and interfacial thermal resistance is neglected. In fact, interfacial thermal resistance between cellulose fibers and the aerogel matrix is neglected due to the absence of experimentally measured interfacial parameters. Perfect thermal continuity is assumed, consistent with conventional homogenization-based finite element modeling approaches for composite materials.

While these effects may influence total TC under extreme thermal conditions or nanoscale interface analyses, they are beyond the scope of the present microscale structural optimization framework. The objective of this work is therefore not to predict the absolute total thermal conductivity including all nanoscale mechanisms, but rather to provide a comparative microscale parametric and optimization framework for structural design guidance.

3. Numerical model

3.1. Governing equations

Heat conduction finite element analyses (FEA) were performed using the commercially available finite element software COMSOL Multiphysics to study micro-scale model under steady-state conditions. The governing equation describing the heat conduction is given by Eq. (1) [34]:

$$\lambda_{xx}\frac{\partial^2 T}{\partial x^2}+\lambda_{yy}\frac{\partial^2 T}{\partial y^2}+\lambda_{zz}\frac{\partial^2 T}{\partial z^2}+(\lambda_{xy}+\lambda_{yx})\frac{\partial^2 T}{\partial x\,\partial y}+(\lambda_{xz}+\lambda_{zx})\frac{\partial^2 T}{\partial x\,\partial z}+(\lambda_{yz}+\lambda_{zy})\frac{\partial^2 T}{\partial y\,\partial z}=0 \quad (1)$$

Where T is the temperature and λ_{xi}, λ_{yi} and λ_{zi} are the directional conductivities in the x, y, and z directions, respectively. The constitutive relation used in the heat conduction model follows Fourier's law, which defines the heat flux vector q as:

$$q=-\lambda\ \nabla T \quad (2)$$

Eqs. (1) and (2) form the basis of the finite-element formulation used to compute the temperature distribution and heat flux within the microscale RVE. These results are then used to determine the ETC components of the CFRA composite along the principal material directions.

3.2. Boundary conditions

To accurately represent the periodic nature of the composite microstructure and ensure continuity of the temperature field across adjacent RVEs, Periodic Boundary Conditions (PBCs) were applied to all opposite faces of the unit cell. These PBCs enforce pointwise temperature compatibility between corresponding nodes on opposing boundaries, thereby preventing artificial discontinuities, fiber separation, or overlap in the periodically repeated microstructure. For each principal direction (x, y and z), a temperature difference of 1 K was imposed between opposite faces while maintaining periodic temperature fluctuations. In other words, the temperature distributions on opposing faces are identical up to a constant offset. This approach enables the evaluation of the ETC in each principal direction without constraining the natural microscopic temperature variations within the RVE.

The PBC formulation used in this study follows the methodology proposed by Xia et al. [35] and subsequently improved by Li et al. [36]. The implementation of these boundary conditions in COMSOL Multiphysics is illustrated in Fig. 2, showing the applied periodic temperature constraints for the RVE model.

3.3. Meshing

In this study, COMSOL Multiphysics was employed to create a free tetrahedral mesh for the RVE. The process of mesh selection underwent rigorous evaluation, incorporating a series of pre-tests encompassing various mesh sizes to pinpoint the most appropriate configuration. Ultimately, a "finer" mesh structure was identified as the optimal choice. Subsequently, further refinements were scrutinized, culminating in the determination that the mesh density best suited for achieving precise and reliable results comprised a total of 67573 individual elements, as precisely outlined in Table S1 of the Supplementary Material. The spatial distribution of this selected mesh configuration for the micro-scale unit cell model is visually depicted in Fig. 3.

4. Results and discussion

4.1. Model validation

To validate the precision of the micro-scale TC calculations, specific mathematical models tailored for UD fiber-reinforced composites were employed, incorporating the fundamental thermal properties of both the fiber and matrix materials. These models facilitated the determination of the thermal conductivities of the yarns under standard ambient conditions, with a temperature denoted as T = 25°C.

The expression governing the axial TC (λ_{ya}) of the yarn within the parallel model [34], which aligns closely with the Rule of Mixture (ROM) concept, is articulated as follows:

$$\lambda_{ya} = \lambda_{f\parallel}\ V_{fy} + \lambda_m\ (1 - V_{fy}) \tag{3}$$

Similarly, the transverse TC λ_{yt} was predicted using the Pilling model [37]:

$$\lambda_{yt} = \lambda_m \left[\frac{\sqrt{(1-V_{fy})^2 \left(\frac{\lambda_{f\perp}}{\lambda_m} - 1\right)^2 + 4\frac{\lambda_{f\perp}}{\lambda_m}} - \left(1 - V_{fy}\right)\left(\frac{\lambda_{f\perp}}{\lambda_m} - 1\right)}{2} \right]^2 \tag{4}$$

The axial and transverse thermal conductivities were also obtained using the Kulkarni and Brady model [38], given by:

$$\lambda_{ya} = \lambda_{f\parallel}\ V_{fy} + \lambda_m\ (1 - V_{fy}) \tag{5}$$

$$\lambda_{yt} = \lambda_m \left[\frac{\lambda_{f\perp}\ (1 + V_{fy}) + \lambda_m\ (1 - V_{fy})}{\lambda_{f\perp}\ (1 - V_{fy}) + \lambda_m\ (1 + V_{fy})} \right] \tag{6}$$

Where $\lambda_{f\parallel}$,$\lambda_{f\perp}$,λ_m are respectively the longitudinal and transverse TCs of the fiber and the TC of the matrix. V_{fy} is the fiber volume fraction in the yarn.

The efficacy of the micromechanical model utilized in this research has been substantiated through prior validation efforts in a study conducted by Wiem et al., specifically addressing aramid fiber-reinforced aerogel composites [39], and the same validation methodology is adopted here.

Table 2 presents a complete comparison between the numerical predictions, experimental results from Jaxel et al. [31], and the analytical models for V_{fy}= 1.3%.

The parallel model (or ROM) [34] was the most accurate of the models tested, with an error of 0% when compared to the simulation result, proving its reliability in forecasting TC under these conditions. Furthermore, the Pilling model [37] and the Kulkarni and Brady model [38] both produced similar forecasts with 0.006% errors, demonstrating their consistency and precision. However, the experimental data exhibited the largest error of 2.32% when compared to the obtained simulation results. In other words, the predictions of models were closer to the simulated values than to the experimental measurements. When choosing the best strategy for particular applications within the field of TC modeling, it is essential to take into account the assumptions and restrictions imposed by each model. It should be noted that comprehensive experimental datasets covering wide ranges of fiber volume fractions and temperature for CFRA systems are currently scarce in the literature. The validation performed in this study is therefore limited to the available experimental reference at low fiber content. While broader validation would be desirable, the present model aims primarily to provide a comparative parametric and optimization framework rather than an exhaustive predictive tool across all operating regimes.

The slightly closer agreement between numerical results and analytical bounds compared to experimental values may be attributed to idealized assumptions in the RVE geometry (uniform fiber distribution and perfect interfacial bonding), whereas experimental samples may exhibit microstructural heterogeneities and imperfect fiber dispersion.

Generally, the comparisons reveal a favorable agreement between our numerical simulations and the experimental data. This level of agreement demonstrates the validity and accuracy of our numerical model in predicting the thermal behavior of the composite material, particularly at lower volume fractions. The axial and transverse TC values differ by only 0.81%, indicating weak anisotropy at this low fiber volume fraction, which is expected since heat transfer is dominated by the aerogel matrix. The distribution of the temperature within the micro-scale unit cell in three local directions is shown in Fig. 4. The data visualization provides an exhaustive understanding of how temperature is distributed inside the RVE.

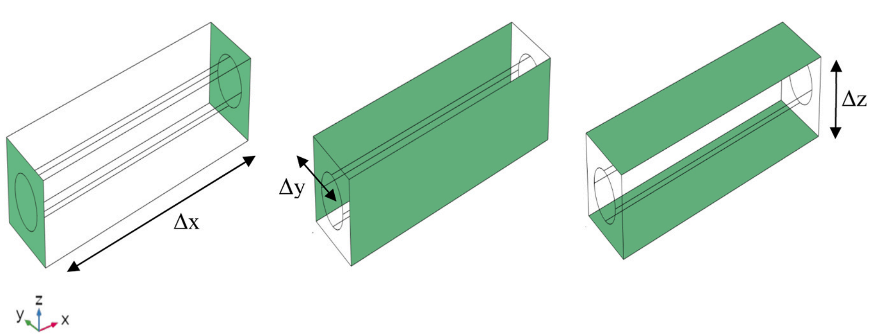

Fig. 2. Periodic boundary conditions.

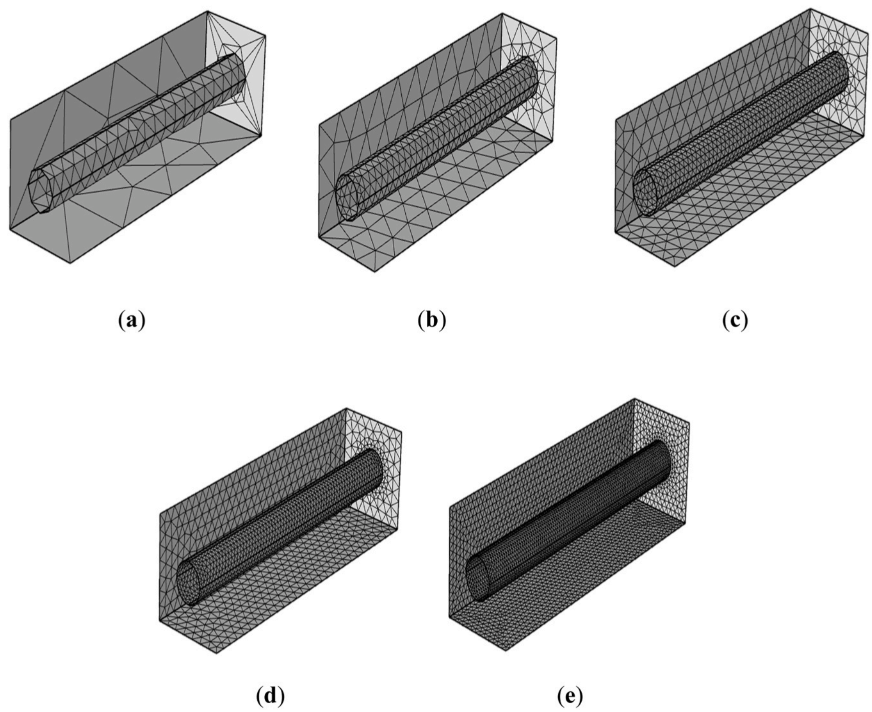

Fig. 3. Meshing with hidden boundaries: (a) extra coarse; (b) normal; (c) finer; (d) extra fine; (e) extremely fine.

Table 2
Model validation: Comparison of thermal conductivities at room temperature between numerical, experimental and analytical models at V_{fy}= 1.3%.

Models	λ_{ya} (W.m^{-1}.K^{-1})	λ_{yt} (W.m^{-1}.K^{-1})	λ_{eff} (W.m^{-1}.K^{-1})	Error (%)
Parallel model	0.016312	-	-	0
Pilling model	-	0.016180	-	0.006
Kulkarni and Brady model	-	0.016180	-	0.006
Experimental	-	-	0.0167 ± 0.0002	2.32
Our simulation	0.016312	0.016179	0.016312	

4.2. Parametric analysis of the effective thermal conductivity

A systematic parametric analysis was conducted to evaluate the influence of the main governing variables on the ETC of CFRA composites. The investigated parameters include fiber volume fraction, temperature, aerogel thermal conductivity, and fiber radius. The corresponding results are summarized in Fig. 5(a–e), where the effect of each parameter is examined while keeping the remaining variables fixed.

The investigated parameter ranges were selected to cover experimentally realistic intervals reported in the literature for CFRAs. Fiber volume fractions between 5% and 40% represent typical reinforcement ranges, while the aerogel conductivity range (0.014–0.023 W·m^{-1}·K^{-1}) corresponds to commonly reported silica aerogel systems. The temperature interval (30–200 °C) was selected to examine performance stability under moderate to elevated thermal conditions relevant to insulation applications.

4.2.1. Impact of the fiber content

It is well known that the fiber content has an immense impact on the thermal properties of the composite [42]. Indeed, the influence of fiber volume fraction on λ_{eff} is illustrated in Fig. 5(a) for different aerogel thermal conductivities at a fixed radius of 13.5 μm. As expected, the ETC increases with increasing fiber content. This can be explained with the increase of the fiber volume fraction and decreasing of the aerogel volume fraction resulting the increasing of the TC of composite. By increasing or decreasing the amount of CFs incorporated into the composite structure during fabrication processes, it becomes possible to control key factors such as TC and specific heat capacity [43]. There is a critical point where high fiber content may negatively affect the thermal properties and degrade insulation performance, especially when radiative and conductive paths become more continuous within the composite [44], no matter how promising they may seem in terms of insulation enhancement aspect. Maintaining an optimal fiber proportion is therefore essential. Furthermore, even with volume fractions of CF that can reach 35% and TCs of aerogel not exceeding 0.021 W.m^{-1}.K^{-1}, it's noteworthy that the ETC of the CFRA remains below that of air at ambient temperature, which stands at 0.026 W.m^{-1}.K^{-1} [31]. This outcome holds significant promise for its insulation properties. The ability to achieve values lower than that of air underscores the exceptional insulating potential of CFRA for a wide range of applications, offering the advantage of energy conservation and enhanced thermal comfort. It also boosts the viability of CFRA as eco-friendly, sustainable materials, aligning with the growing demand for green and energy efficient solutions in various industries [45].

4.2.2. Impact of the temperature

Temperature plays a significant role in governing the global heat-transfer response of CFRA composites through the imposed thermal gradient across the RVE. In the present simulations, the intrinsic thermal conductivities of both the aerogel matrix and the CFs were assumed constant over the investigated temperature range in order to isolate parametric effects and ensure numerical stability. Consequently, temperature in this model acts primarily as an external loading parameter influencing the overall heat flux rather than introducing nonlinear material property variation.

Figs. 5(b) and 5(c) present the variation of the ETC with temperature for different aerogel intrinsic conductivities and fiber volume fractions, respectively. In both cases, the ETC exhibits a clear increasing trend with temperature, with a slightly nonlinear response at higher temperature levels. Within the framework of constant material properties, this behavior reflects the amplified heat flux associated with higher applied

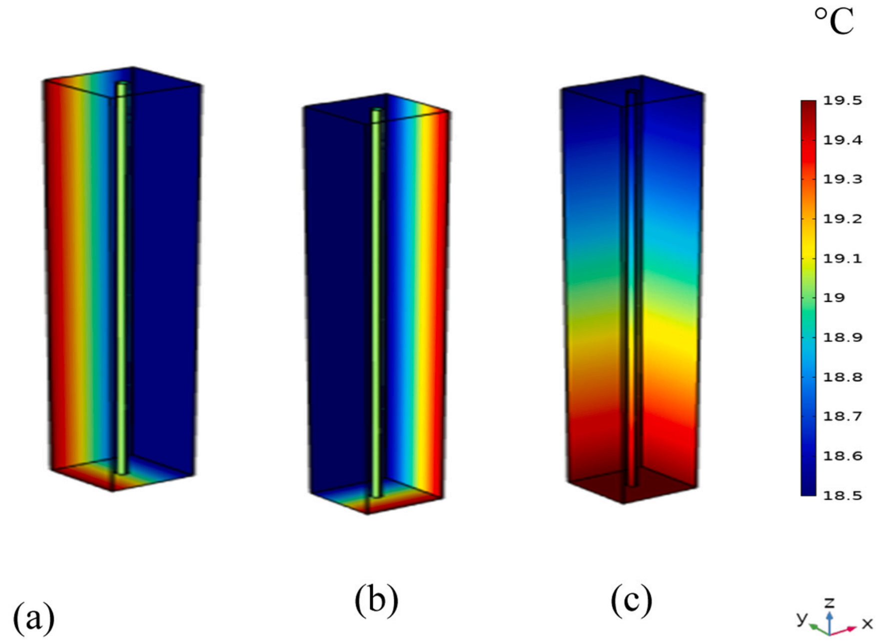

Fig. 4. Temperature distributions with hidden boundaries in the three local coordinate directions: (a) T_x; (b) T_y; **(c)** T_z.

thermal gradients and the interaction between temperature and other microstructural parameters captured by the quadratic response surface model.

From a physical standpoint, real CFRA systems exhibit temperature-dependent thermal transport mechanisms. For CFs and silica aerogels, heat transfer within the solid phase is largely governed by phonon-mediated conduction. As temperature increases, enhanced lattice vibrations promote more efficient energy transfer through the solid skeleton of both the aerogel network and the cellulose fibers. In highly porous aerogels, temperature may also influence gas-phase conduction within pores and modify phonon–gas scattering effects, contributing to a gradual increase in ETC. Experimental studies on cellulose-based aerogels and hygroscopic fibrous materials report similar temperature-dependent trends in TC [46]. Although such intrinsic temperature dependence was not explicitly modeled in the present work, the observed increase in ETC remains consistent with established thermophysical behavior reported for bio-based aerogel composites [46].

Despite the increase in ETC with temperature, the computed values remain within the low-conductivity domain characteristic of super-insulating materials over the entire examined range. This confirms the robustness of CFRA composites for thermal insulation and thermal management applications under variable thermal environments, particularly when low-conductivity aerogels and moderate fiber volume fractions are employed.

4.2.3. Impact of the thermal conductivity of aerogel

A range of aerogel TC values was considered in this study, varying between 0.014 and 0.023 $W \cdot m^{-1} \cdot K^{-1}$, to evaluate their influence on the global thermal performance of the CFRA composite. As illustrated in Fig. 5(d), the ETC of the composite increases steadily as the conductivity of the aerogel matrix increases, regardless of the fiber volume fraction. This behavior is expected, since the aerogel constitutes the continuous phase of the composite and therefore provides the primary pathway for heat transfer [31]. When the aerogel exhibits a lower intrinsic TC, heat propagation through the matrix is more strongly impeded, enabling the composite to retain its super-insulating characteristics. Conversely, as the aerogel conductivity increases, the solid backbone of the matrix becomes more conductive, which directly elevates the ETC of the composite. The nearly linear relationship observed in Fig. 5(d) confirms that the aerogel matrix dominates the heat-transfer mechanism, while the contribution of cellulose fibers remains secondary within the studied range. This finding highlights the critical importance of selecting or engineering aerogels with ultra-low conductivity values when designing CFRA composites for high-performance thermal insulation applications.

4.2.4. Impact of the fiber radius

The radius of CFs can vary significantly depending on the botanical source and the processing techniques employed during their extraction, typically falling within the range of 10–50 μm [10]. Fig. 5(e) illustrates the influence of fiber radius on the ETC of the CFRA composite within the investigated domain. The results show that increasing the fiber radius from 10 μm to 17 μm produces only a very slight decrease approximately 0.08% in the ETC. This minimal change indicates that, within this radius interval, the fiber size has a negligible effect on overall heat transfer in the composite [47].

This weak sensitivity can be attributed to the fact that the aerogel matrix, rather than the fibers, governs the primary thermal transport mechanism in CFRA composites [44]. Because the matrix possesses an intrinsically ultra-low TC and occupies the majority of the composite volume at low fiber fractions, modifications in fiber dimensions do not significantly perturb the global heat-transfer pathways [47]. As a result, other parameters such as temperature, fiber volume fraction, and aerogel thermal conductivity exert a much stronger influence on ETC compared to fiber radius. These findings suggest that modest variations in CF dimensions during manufacturing are unlikely to compromise the thermal insulation performance of CFRA composites [43].

4.3. DOE using response surfaces method

Response Surface Methodology (RSM), a collection of statistical and mathematical techniques for process optimization, provides a structured framework for analyzing how multiple input parameters influence a response of interest. When coupled with a Design of Experiments (DOE) approach, RSM enables the development of predictive models, identification of key factors, and optimization of complex engineering systems with a reduced number of simulations or experiments. In this work, RSM served three specific purposes: to identify which parameters significantly influence the effective thermal conductivity, to quantify interaction effects between parameters, and to establish a predictive model for optimization without running additional computationally expensive

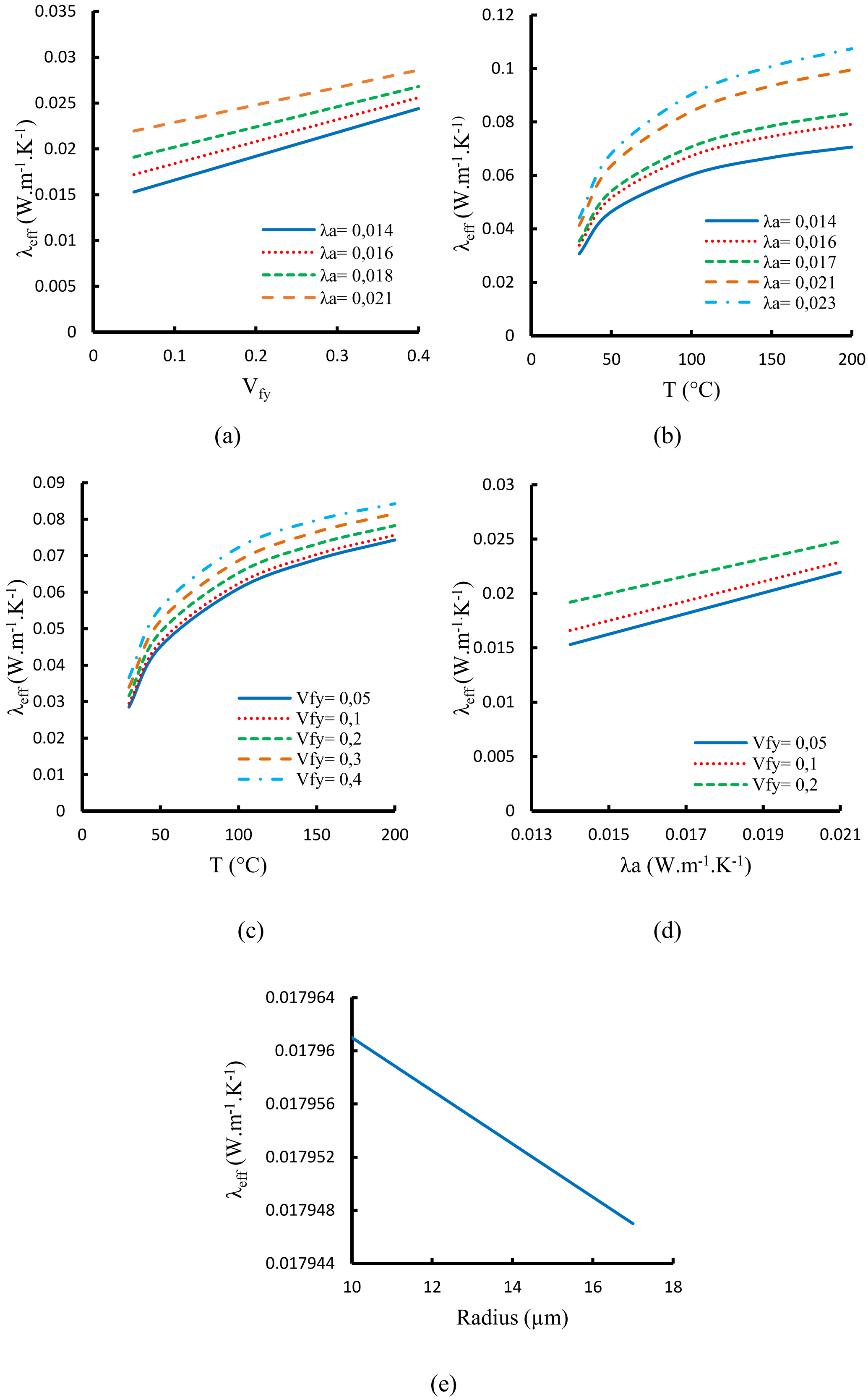

Fig. 5. Parametric influence on the ETC of CFRA composites: (a) effect of fiber volume fraction for different aerogel conductivities (R = 13.5 μm); (b) temperature effect for varying aerogel conductivities (R = 13.5 μm, V_{fy} = 35.75%); (c) temperature effect for varying fiber volume fractions (R = 13.5 μm, λ_a = 0.017 W.m^{-1}.K^{-1}); (d) effect of aerogel thermal conductivity for different fiber volume fractions (R = 13.5 μm); (e) effect of fiber radius (V_{fy} = 1.3%, λ_a = 0.017 W.m^{-1}.K^{-1}).

simulations. To this end, the combined effects of four governing parameters; temperature, fiber volume fraction, fiber radius, and aerogel TC on the ETC of CFRA composites were quantified and optimized. A Box Behnken design (BBD) was selected over other designs (e.g., central composite design (CCD)) because it requires fewer runs for four factors (27 runs versus 30 for CCD) while still providing sufficient information for fitting a quadratic model. BBD also avoids extreme factor combinations where all factors are simultaneously at their highest or lowest levels, which may correspond to physically unrealistic material configurations. Accordingly, each factor was varied over three equally spaced levels (coded as −1, 0, +1), as shown in Table 3, enabling efficient estimation of linear, quadratic, and two-way interaction effects while ensuring a thorough exploration of the design space.

The quadratic regression equation linking those parameters to the desired ETC is given as:

$$\lambda_{eff} = -0.026 + 0.000454\ T + 0.02781\ V_{fy} + 2.1897\ \lambda_a - 0.000113\ R - 0.000002\ T^2 + 0.000029\ {V_{fy}}^2 + 0.01546\ {\lambda_a}^2 + 0.00872\ R^2 - 0.05749\ T\ V_{fy} - 0.014\ T\ \lambda_a - 0.000139\ T\ R - 1.3957\ V_{fy}\ \lambda_a + 0.00148\ V_{fy}\ R - 0.00013\ \lambda_a\ R \quad (7)$$

The resulting quadratic regression model captures the combined influence of the four input parameters on the ETC of the composite. The coefficients were obtained through least-squares fitting of the simulation data generated using the Box–Behnken design. Table S2 of the Supplementary Material summarizes all DOE runs, showing the combinations of the four continuous factors and the corresponding ETC values computed for each case. This structured design ensures an efficient and balanced exploration of the design space while minimizing the number of required simulations.

The regression model was evaluated using analysis of variance (ANOVA) based on the 27-run Box–Behnken design. The statistical analysis demonstrated excellent model performance, with a coefficient of determination R^2= 0.9976 and an adjusted coefficient R^2_{adj}= 0.9948. The high R^2 value indicates that 99.76% of the variability in ETC is explained by the proposed quadratic model, while the close agreement between R^2 and adjusted R^2 confirms that the model maintains strong predictive capability without evidence of overfitting. Furthermore, the model F-value of 356.47, combined with an extremely small p-value ($p < 0.0001$), demonstrates that the regression is statistically significant and that the relationship between the selected design variables and ETC is highly reliable within the investigated parameter space.

It should be noted that, since the finite element simulations are deterministic in nature, replicated center-point runs produced identical responses, resulting in zero pure error variance. Consequently, the classical lack-of-fit test cannot be computed because the denominator of the test statistic becomes mathematically undefined. This outcome is expected in simulation-based design studies and does not reflect any inadequacy of the regression model, but rather the absence of experimental noise in numerically generated data.

In this model, temperature T was observed to vary between 30°C and 200°C, demonstrating a significant influence on λ_{eff}. When all other factors were held constant, increasing the temperature from 30 °C to 200 °C lead to a noticeable increase in λ_{eff}, as seen in rows 1 and 2 (from 0.03094 $W.m^{-1}.K^{-1}$ to 0.08074 $W.m^{-1}.K^{-1}$) and rows 9 and 10 (from 0.03453 $W.m^{-1}.K^{-1}$ to 0.08473 $W.m^{-1}.K^{-1}$). While, the fiber volume fraction V_{fy} values ranged from 0.05 to 0.4, its impact is moderate as showing in rows 1 and 3 and it has less effect on λ_{eff} than temperature. The values of aerogel thermal conductivity λ_a, at 0.014 and 0.023, displayed varying effects on λ_{eff} across different runs. Rows 5 and 6 indicated that increasing λ_a resulted in higher λ_{eff}, but this effect was not consistent. Lastly, the radius of cellulose fiber R, ranging from 10 μm to 17 μm, had a relatively minor impact on λ_{eff}, with only slight variations observed in rows 5 and 7 (0.05770 $W.m^{-1}.K^{-1}$ and 0.05796 $W.m^{-1}.K^{-1}$).

The relative contributions of the investigated parameters to the ETC were quantified from the ANOVA results. Temperature was identified as the dominant factor, accounting for approximately 40–45% of the total variation in ETC, followed by the intrinsic thermal conductivity of the aerogel matrix, which contributed roughly 35–40%. The fiber volume fraction exhibited a moderate influence, representing about 10–15% of the variability, whereas the fiber radius had a comparatively minor effect, contributing less than 5%. Interaction effects between variables collectively accounted for approximately 10–15% of the total response variation.

These results confirm that the thermal behavior of the composite is primarily governed by matrix-controlled conduction mechanisms, with geometric parameters playing a secondary role. The strong influence of temperature observed in the statistical analysis reflects the imposed thermal loading conditions and the dominant contribution of the aerogel matrix as the continuous phase within the RVE. Since the aerogel constitutes the majority of the composite volume, variations in the applied temperature field directly affect the overall heat flux distribution and, consequently, the ETC response.

In contrast, the influence of fiber radius within the investigated range (10–17 μm) remains limited because the fiber volume fraction was varied independently, and the selected radius interval does not significantly alter the overall conductive path geometry at the microscale. Classical effective medium theories, such as Maxwell–Eucken-type formulations, indicate that inclusion size does not explicitly affect effective conductivity in the absence of interfacial thermal resistance [48]. This theoretical prediction explains the weak sensitivity observed in the present simulations. Since heat transfer is assumed to be conduction-dominated and perfect interfacial bonding is considered, geometric scaling effects associated with fiber curvature remain secondary.

Overall, the observed trends are consistent with micromechanical scaling principles, whereby effective conductivity is primarily governed by intrinsic phase conductivity and phase volume fraction rather than moderate variations in inclusion radius under ideal interfacial conditions.

The obtained regression model provides a practical tool for predicting and optimizing the ETC of CFRA composites within the studied design space. In addition, the model can be directly used as an input parameter for macroscale thermal simulations, offering an efficient link between microscale modeling and engineering-scale applications

Table 3
Levels of process parameters.

Parameters	Levels		
	-1	0	1
Temperature (°C)	30	115	200
Fiber volume fraction	0.05	0.225	0.4
Thermal conductivity of Aerogel ($W.m^{-1}.K^{-1}$)	0.014	0.0185	0.023
Radius of Cellulose fiber (μm)	10	13.5	17

5. Conclusion

This work established a rigorous microscale computational statistical framework for predicting and optimizing the ETC of CFRA composites. Through three-dimensional periodic homogenization and systematic design of experiments (BBD with 27 simulations), the study quantitatively clarified the relative contributions of microstructural and thermal parameters across a design space defined by fiber volume fraction, fiber radius, aerogel thermal conductivity, and temperature

The results confirm that heat transfer in CFRA systems is primarily governed by matrix-controlled conduction mechanisms. Within the investigated range, temperature exhibited the strongest influence on ETC, leading to a substantial increase in ETC as thermal loading increased. Aerogel intrinsic conductivity contributed 35–40% of the total response variability, while fiber volume fraction exhibited a moderate influence (10–15% contribution). Notably, fiber radius variations within manufacturing-relevant ranges (10–17 μm) remained thermally insignificant (< 0.1% variation) under ideal interfacial conditions, a finding consistent with effective medium theory that enables relaxed manufacturing tolerances and cost-effective production using commercially available cellulose fibers.

Optimization identified the ideal microstructural configuration; 1.3% fiber volume fraction, 7 μm fiber radius, and 0.016 $W.m^{-1}.K^{-1}$ aerogel conductivity, yielding an ETC of 0.0163 $W.m^{-1}.K^{-1}$ at room temperature. This value is 37% lower than the thermal conductivity of air (0.026 $W.m^{-1}.K^{-1}$) and well within the super-insulating material range, demonstrating that minimal cellulose fiber reinforcement can enhance structural integrity without compromising exceptional insulation performance.

The quadratic regression model demonstrated excellent statistical performance ($R^2 = 0.9976$, adjusted $R^2 = 0.9948$, F-value = 356.47, $p < 0.0001$), confirming the effectiveness of coupling finite-element micromechanics with RSM for design-oriented analysis. Beyond parametric interpretation, the developed predictive model provides a practical tool for guiding material selection and microstructural tailoring. The findings suggest that maintaining low fiber contents, prioritizing ultra-low conductivity aerogels, and allowing reasonable variability in fiber dimensions can collectively support high-performance and cost-effective CFRA insulation designs.

This integrated methodology serves as a bridge between predictive design and experimental characterization, establishing a scalable platform for advancing sustainable bio-based thermal insulation systems. Future work should extend this framework to incorporate interfacial thermal resistance, temperature-dependent material properties, and coupled heat-moisture transport for comprehensive multi-physics optimization of CFRA composites for energy-efficient buildings and thermal management applications.

CRediT authorship contribution statement

Mabrouk Mosbahi: Visualization, Validation, Supervision, Software, Resources. **Ridha Djebali:** Visualization, Supervision, Resources. **Khaled Gammoudi:** Visualization, Validation, Supervision, Resources. **Tullio Tucciarelli:** Supervision, Software, Methodology. **Wiem Nasri:** Writing – review & editing, Writing – original draft, Methodology, Funding acquisition, Formal analysis. **Sondes Ifa:** Resources, Methodology, Investigation. **Marwa Hannachi:** Supervision, Software, Investigation. **Abderazak Bezazi:** Validation, Supervision, Project administration. **Reis Paulo:** Formal analysis, Data curation, Conceptualization. **Zied Driss:** Visualization, Supervision, Formal analysis.

Author contributions

W.N.: Conceptualization, Data curation, Formal analysis, Investigation, Methodology, Software, Validation, Visualization, Writing original draft, Review and editing; Z.D., P.R: Supervision, review & editing; R.D.: DOE optimization; M.H., S.I., M.M., A.B., K.G.: Review & editing; M.M., T.T.: Funding acquisition. All authors have read and agreed to the published version of the manuscript.

Ethical approval

'Not Applicable'.

Informed consent statement

'Not applicable'.

Institutional review board statement

'Not applicable'.

Declaration of Generative AI and AI-assisted technologies in the writing process

'Not applicable'.

Funding

This research was sponsored by University of Palermo.

Declaration of Competing Interest

The authors declare that they have no known competing financial interests or personal relationships that could have appeared to influence the work reported in this paper.

Appendix A. Supporting information

Supplementary data associated with this article can be found in the online version at doi:10.1016/j.mtcomm.2026.114947.

Data availability

No data was used for the research described in the article.

References

[1] A. Bakatovich, F. Gaspar, Composite material for thermal insulation based on moss raw material, Constr. Build. Mater. 228 (2019) 116699.
[2] A.M. Papadopoulos, State of the art in thermal insulation materials and aims for future developments, Energy Build. 37 (1) (2005) 77–86.
[3] A. Cosentino Garcia Miguel, F.C. Silva, G. da Silva, J. Sciamareli, E.A. da Costa Mattos, Short review about aerospace materials characterization–bonding agents and thermal insulation, Propellants Explos. Pyrotech. 45 (8) (2020) 1175–1184.
[4] J.E. Fesmire, Layered composite thermal insulation system for nonvacuum cryogenic applications, Cryogenics 74 (2016) 154–165.
[5] K. Aruchamy, S.K. Palaniappan, M. Velusamy, et al., Hybridization of cotton/bamboo woven fabric epoxy composite laminates: an experimental investigation and optimization, Discov. Mater. (2025).
[6] M.B. Khan, M. Umer, P.O. Awoyera, et al., Optimization of mechanical and durability performance of graphene nanoplatelet modified PVA fiber reinforced cementitious composites using response surface methodology, Sci. Rep. (2026).
[7] G. Boukhatem, M. Bencheikh, S.R. Bekkouche, et al., Data-driven optimization and pressuremeter modulus prediction using response surface methodology for smarter geotechnical design, Sci. Rep. (2026).
[8] M.Ş. Adin, H. Adin, Machining eco-friendly jute fiber-reinforced epoxy composites using specially produced cryo-treated and untreated cutting tools, Polymers 16 (2024) 3329.
[9] G. Yadav, R. Srinivas, N. Gupta, et al., Sustainable shape formation of multifunctional carbon fiber-reinforced polymer composites: a study on recent advancements, Mech. Adv. Mater. Struct. 31 (26) (2024).
[10] G. Chinga-Carrasco, Cellulose fibres, nanofibrils and microfibrils: the morphological sequence of MFC components from a plant physiology and fibre technology point of view, Nanoscale Res. Lett. 6 (2011) 1–7.
[11] H. Chakhtouna, H. Benzeid, N. Zari, A.E.K. Qaiss, R. Bouhfid, Recent advances in eco-friendly composites derived from lignocellulosic biomass for wastewater treatment, Biomass Convers. Biorefinery 14 (11) (2024) 12085–12111.
[12] R.K. Pal, P. Goyal, S. Sehgal, Effect of cellulose fibre based insulation on thermal performance of buildings, Mater. Today. Proc. 45 (2021) 5778–5781.
[13] Y. Chen, L. Gan, Y. Dai, H. Shi, T. Zhang, F. Qiu, D. Yang, Transparent cellulose-based film with water resistance and thermal protective for agriculture application, Biomass Convers. Biorefinery 14 (20) (2024) 25973–25983.

[14] P. Itkor, A.K. Singh, M. Lee, A. Boonsiriwit, Y.S. Lee, Effects of starch–citric acid cross-linking on the fibrous composites using waste paper pulp material for eco-friendly packaging, Biomass Convers. Biorefinery 14 (13) (2024) 14693–14705.

[15] J.L. Gurav, I.K. Jung, H.H. Park, E.S. Kang, D.Y. Nadargi, Silica aerogel: synthesis and applications, J. Nanomater. 2010 (1) (2010) 409310.

[16] A.S. Dorcheh, M.H. Abbasi, Silica aerogel; synthesis, properties and characterization, J. Mater. Process. Technol. 199 (1-3) (2008) 10–26.

[17] S. Chandrasekaran, D. Lin, Y. Li, M.A. Worsley, Aerogels, additive manufacturing, and energy storage, Joule 7 (5) (2023) 866–883.

[18] S. Singh, A. Bhatnagar, V. Dixit, V. Shukla, M.A. Shaz, A.S.K. Sinha, O. N. Srivastava, V. Sekkar, Synthesis, characterization and hydrogen storage characteristics of ambient pressure dried carbon aerogel, Int. J. Hydrogen Energy 41 (5) (2016) 3561–3570.

[19] T. Kim, V.G. Parale, H.N.R. Jung, Y. Kim, Z. Driss, D. Driss, A. Bouabidi, S. Euchi, H.H. Park, Facile synthesis of SnO2 aerogel/reduced graphene oxide nanocomposites via in situ annealing for the photocatalytic degradation of methyl orange, Nanomaterials 9 (3) (2019) 358.

[20] J. Zhao, C. Lu, X. He, X. Zhang, W. Zhang, X. Zhang, Polyethylenimine-grafted cellulose nanofibril aerogels as versatile vehicles for drug delivery, ACS Appl. Mater. Interfaces 7 (4) (2015) 2607–2615.

[21] C. Buratti, E. Moretti, E. Belloni, Aerogel plasters for building energy efficiency. Nano and biotech based materials for energy building efficiency, Springer, 2016, pp. 17–40.

[22] J.P. Randall, M.A.B. Meador, S.C. Jana, Tailoring mechanical properties of aerogels for aerospace applications, ACS Appl. Mater. Interfaces 3 (3) (2011) 613–626.

[23] Y. Yu, Z. Zhuang, W. Zhang, et al., Cellulose-based aerogel fibers with enhanced mechanical properties for thermal insulation and humidity response, Int. J. Biol. Macromol. (2025) 147053.

[24] M. Huang, C. Zhang, Y. Zhan, et al., Foam-formed aramid aerogels reinforced by nanocellulose: distinct roles of bacterial and carboxylated cellulose nanofibers in tailoring strength and thermal insulation, J. Colloid Interface Sci. (2025) 139710.

[25] Y. Xiang, Y. Hu, W. Yu, et al., Kenaf cellulose nanofiber-based aerogel loading and sustained-release cinnamon essential oil for chilled pork preservation, LWT (2025) 118927.

[26] W.-N. Xu, M.-H. Wang, T. Liu, et al., Highly flexible cellulose-silica composite aerogels from hemp straw, Ind. Crops Prod. 239 (2026) 122511.

[27] H. Adin, M. Adin, Effect of particles on tensile and bending properties of jute epoxy composites, Mater. Test. 64 (3) (2022) 401–411.

[28] C. Rudaz, A. Demilecamps, G. Pour, M. Alves, A. Rigacci, H. Sallee, G. Reichenauer, T. Budtova, Bio-based aerogels: a new generation of thermal super-insulating materials. EMN (Energy, Materials, Nanotechnology) Meeting on Polymer, 2015.

[29] Y. Kobayashi, T. Saito, A. Isogai, Aerogels with 3D ordered nanofiber skeletons of liquid-crystalline nanocellulose derivatives as tough and transparent insulators. Angew. Chem. Int. Ed. 53 (39) (2014) 10394–10397.

[30] C. Jiménez-Saelices, B. Seantier, B. Cathala, Y. Grohens, Spray freeze-dried nanofibrillated cellulose aerogels with thermal superinsulating properties, Carbohydr. Polym. 157 (2017) 105–113.

[31] J. Jaxel, G. Markevicius, A. Rigacci, T. Budtova, Thermal superinsulating silica aerogels reinforced with short man-made cellulose fibers, Compos.Part A Appl. Sci. Manuf. 103 (2017) 113–121.

[32] Z. Shao, X. He, Z. Niu, T. Huang, X. Cheng, Y. Zhang, Ambient pressure dried shape-controllable sodium silicate based composite silica aerogel monoliths, Mater. Chem. Phys. 162 (2015) 346–353.

[33] R. Baetens, B.P. Jelle, A. Gustavsen, Aerogel insulation for building applications: a state-of-the-art review, Energy Build. 43 (4) (2011) 761–769.

[34] K. Dong, K. Liu, Q. Zhang, B. Gu, B. Sun, Experimental and numerical analyses on the thermal conductive behaviors of carbon fiber/epoxy plain woven composites, Int. J. Heat. Mass Transf. 102 (2016) 501–517.

[35] Z. Xia, Y. Zhang, F. Ellyin, A unified periodical boundary conditions for representative volume elements of composites and applications, Int. J. Solids Struct. 40 (8) (2003) 1907–1921.

[36] S. Li, Boundary conditions for unit cells from periodic microstructures and their implications, Compos. Sci. Technol. 68 (9) (2008) 1962–1974.

[37] M.W. Pilling, B. Yates, M.A. Black, P. Tattersall, The thermal conductivity of carbon fiber-reinforced composites, J. Mater. Sci. 14 (1979) 1326–1338.

[38] M.R. Kulkarni, R.P. Brady, A model of global thermal conductivity in laminated carbon/carbon composites, Compos. Sci. Technol. 57 (3) (1997) 277–285.

[39] W. Nasri, R. Djebali, A.J. Chamkha, A. Bezazi, F. Mechighel, P. Reis, Z. Driss, Thermal behavior of mesoporous aramid fiber reinforced silica aerogel composite for thermal insulation applications: microscale modeling, J. Appl. Comput. Mech. 10 (1) (2024) 140–151.

[40] M. Antlauf, N. Boulanger, L. Berglund, K. Oksman, O. Andersson, Thermal conductivity of cellulose fibers in different size scales and densities, Biomacromolecules 22 (9) (2021) 3800–3809.

[41] T. Hatakeyama, K. Nakamura, H. Hatakeyama, Studies on heat capacity of cellulose and lignin by differential scanning calorimetry, Polymer 23 (12) (1982) 1801–1804.

[42] S. Rajendran, G. Palani, H. Trilaksana, U. Marimuthu, G. Kannan, Y.L. Yang, V. Shanmugam, Advancements in natural fibre based polymeric composites: a comprehensive review on mechanical-thermal performance and sustainability aspects, Sustain. Mater. Technol. 44 (2025) e01345.

[43] S. Jiang, S. Jiang, J. Yan, C. Lin, W. Wang, S. Jiang, L. Cao, R. Guo, In situ cross-linking reinforced cellulose aerogel fibers for thermal insulation and multifunctional applications, Ind. Eng. Chem. Res. 63 (34) (2024) 15301–15313.

[44] R.A. Hansel, J. Rozen, D.G. Walker, Transport involving conducting fibers in a non-conducting matrix, Int. J. Therm. Sci. 49 (9) (2010) 1561–1566.

[45] L. Ma, H. Wu, Y. Wei, L. Zhu, Y. Li, Y. Zhong, L. Li, Z. Tan, C. Yun, Q. Zhang, X. Wei, Z. Zhang, S. Ramakrishna, C. Liu, Reinforcement strategies for cellulose-based aerogels from textile waste and their applications in thermal insulation and oil absorption, Int. J. Biol. Macromol. 308 (2025) 142526.

[46] V. Apostolopoulou-Kalkavoura. Thermal conductivity of hygroscopic foams based on cellulose nanomaterials, Stockholm University, 2021. PhD Thesis.

[47] R. Sharma, V.K. Gaba, S.I. Kundalwal, R. Suresh Kumar, Estimation of thermal properties of fuzzy carbon fiber heat exchanger using micromechanics approach, J. Indian Chem. Soc. 97 (7) (2020) 1169–1177.

[48] M. Zain-ul-Abdein, W.S. Awan, H. Ijaz, et al., Effect of micro-to nanosize inclusions upon the thermal conductivity of powdered composites with high and low interface resistance, J. Nanomater. 2015 (1) (2015) 843914.